Novel D-π-A and A-π-D-π-A Three-Component Photoinitiating Systems Based on Carbazole/Triphenylamino based Chalcones and Application in 3D and 4D Printing

Hong Chen, Guillaume Noirbent, Yijun Zhang, Damien Brunel, Didier Gigmes, Fabrice Morlet-Savary, Bernadette Graff, Pu Xiao, Frédéric Dumur, Jacques Lalevée

Novel D-π-A and A-π-D-π-A Three-Component Photoinitiating Systems Based on Carbazole/Triphenylamino based Chalcones and Application in 3D and 4D Printing

Hong Chen [1,2], Guillaume Noirbent [3], Yijun Zhang [1,2], Damien Brunel [3], Didier Gigmes[3], Fabrice Morlet-Savary [1,2], Bernadette Graff [1,2], Pu Xiao [4*], Frédéric Dumur [3*], Jacques Lalevée [1,2*]

[1] Université de Haute-Alsace, CNRS, IS2M UMR 7361, F-68100 Mulhouse, France
[2] Université de Strasbourg, France
[3] Aix Marseille Univ, CNRS, ICR UMR 7273, F-13397 Marseille, France; frederic.dumur@univ-amu.fr
[4] Research School of Chemistry, Australian National University, Camberra, ACT 2601, Australia; pu.xiao@anu.edu.au
* Corresponding author: jacques.lalevee@uha.fr (J. L.), frederic.dumur@univ-amu.fr (F. D.); pu.xiao@anu.edu.au (P. X.).

Abstract: A series of carbazole or triphenylamine based mono-chalcones, displaying either D-π-A or A-π-D-π-A architecture, have been designed and synthesized for intense absorption bands at around 405 nm with high molar extinction coefficients around 10^5 $M^{-1}cm^{-1}$ corresponding to π-π* electronic transitions. Photosensitivity of the new photoinitiating systems composed of a chalcone and an iodonium salt (Iod) was investigated by UV-visible absorption and fluorescence spectroscopies, and their photoinitiation abilities were examined during the free radical polymerization of acrylates, whose polymerization kinetics were monitored by real-time Fourier Transform Infrared (RT-FTIR) spectroscopy upon irradiation with a LED@405nm. In this work, a series of ten chalcones comprising a carbazole unit or a triphenylamine (TPA) group used as the electron donor for chalcones were specifically designed. Remarkably, nine of the proposed chalcones were never reported in literature (never synthesized before). Only chalcone 7 was reported but only as a precursor for the design of pyrazolines for optical materials. As a result of this strategy, highly conjugated high-molecular-weight photoinitiators were obtained, displaying improved light absorption properties due to their extended polyaromaticity. These new photoinitiators open new perspectives for the design of novel and efficient photoinitiators. To evidence the interest of these new chalcones, 3D and 4D printing experiments were carried out with a polyethylene glycol (PEG)-diacrylate photosensitive resin comprising the best photoinitiating systems investigated. The

shapes of 3D patterns can be reversibly modified by mean of a thermal or hydrophilic response of PEG for a 4D activation.

Keywords: chalcone, free radical polymerization, 3D printing, reversible deformation effect, 4D printing.

1.Introduction

Photoinitiated free radical polymerization is a valuable technique for the *in-situ* formation of hydrogels as it provides an unparalleled spatial and temporal control over the formation of polymers under mild reaction conditions [1-4]. In general, applications of this polymerization technique are widespread due to the fact that the polymerization reaction is temporarily controlled and can be initiated on demand, what can be advantageously used in industry for applications such as inks, coatings, adhesives, varnishes and microelectronics [5-8], and various biomedical applications [9-10]. An efficient photoinitiator (PI) plays an essential role in the photopolymerization process, which induces the rapid conversion of liquid monomers into highly crosslinked solid polymers by absorbing the appropriate wavelengths of light and generate reactive species (e.g. cations, free radicals, anions…) [11-13]. Nevertheless, the majority of the commercially available photoinitiators remains UV light sensitive. In this context, the design and synthesis of highly efficient photoinitiating systems applicable for visible light sources such as light-emitting diodes (LEDs) are of great interest but still remain a challenge. Besides, visible light sources such as LEDs are appealing candidates for industrial applications due to their lower price, low energy consumption offering safe operating conditions to the manipulators [14-15].

In our previous studies, we have demonstrated that several chalcones combined with an iodonium salt and an amine can act as suitable three-component photoinitiating systems (PISs) which present good near UV, visible light absorption properties and high efficiencies for the photopolymerization of acrylates under a LED@405 nm [16-17]. However, most of the PISs based on chalcone/Iod/amine exhibit less-than-perfect performance upon LED irradiation as these compounds have a maximum absorbance below 365 nm where the most common and cost-effective UV/LED lamps irradiate. Hence, in the present study, we wish to improve the absorption properties of chalcones including a red-shifted absorption and high molar

extinction coefficients by introducing carbazole or triphenylamine (TPA) groups in the molecular structures [18-19].

Chalcones are a class of natural compounds present in many plants, which has attracted a widespread attention owing to a variety of physiological activities (e.g., anti-tumor, anti-inflammatory, anti-bacterial, anti-oxidation, etc.) [20-25]. In addition, due to the highly conjugated nature of the framework structure, chalcones exhibit good optical properties and UV-photosensitivity, which is an ideal class of nonlinear optical materials [16,26-27]. Apart from that, carbazole is an electron donor with a rigid, fully conjugated and planar structure, which has been extensively used in organic electronics due to its facile oxidation and its good hole-transport ability [28-29]. This group has also been extensively used for the design of photoinitiators due to its interesting photophysical properties for radical chemistry [30-37]. Furthermore, triphenylamine (TPA) is one of the most applied electron donors in the design of organic dipolar chromophores and hole-transport materials for organic light-emitting diodes (OLEDs) [38-41]. When introducing a carbazole or TPA group into chalcone to form D-π-A or A-π-D-π-A (where D and A stand for donor and acceptor respectively) structures, an efficient intramolecular charge transfer (ICT) in the excited state can be observed. Considering that carbazoles and triphenylamines are excellent electron donors, the push-pull effect caused by the intramolecular interactions between the donor and the acceptor will lead to a strong charge delocalization all over the molecule, thus inducing the appearance of an intense transition in the visible region [42-44].

In this paper, we designed and synthesized a series of 10 different carbazole or TPA-based chalcones with good visible light absorption properties which were predicted by molecular modeling design. It has to be noticed that among the series of ten chalcones proposed in this work, nine of them have never been reported in literature, and only chalcone 7 was used as a precursor for the design of pyrazolines [45]. Furthermore, the synthesized chalcones were used as photoinitiators and combined with a co-initiator (iodonium salt) to form novel two-component PISs. The optical, electrochemical and theoretical properties of these compounds were studied using time-resolved Fourier Transform InfraRed (TR-FTIR) spectroscopy, UV-visible absorption, fluorescence spectroscopy, cyclic voltammetry as well as electron spin resonance (ESR) experiments or molecular modeling data. In addition, excellent tridimensional (3D) patterns could be obtained by using the newly proposed

two-component PISs for 3D printing experiments. Remarkably, reversible deformation effects on these 3D objects can be stimuli controlled (by hydration or heat) leading to 4D printing applications.

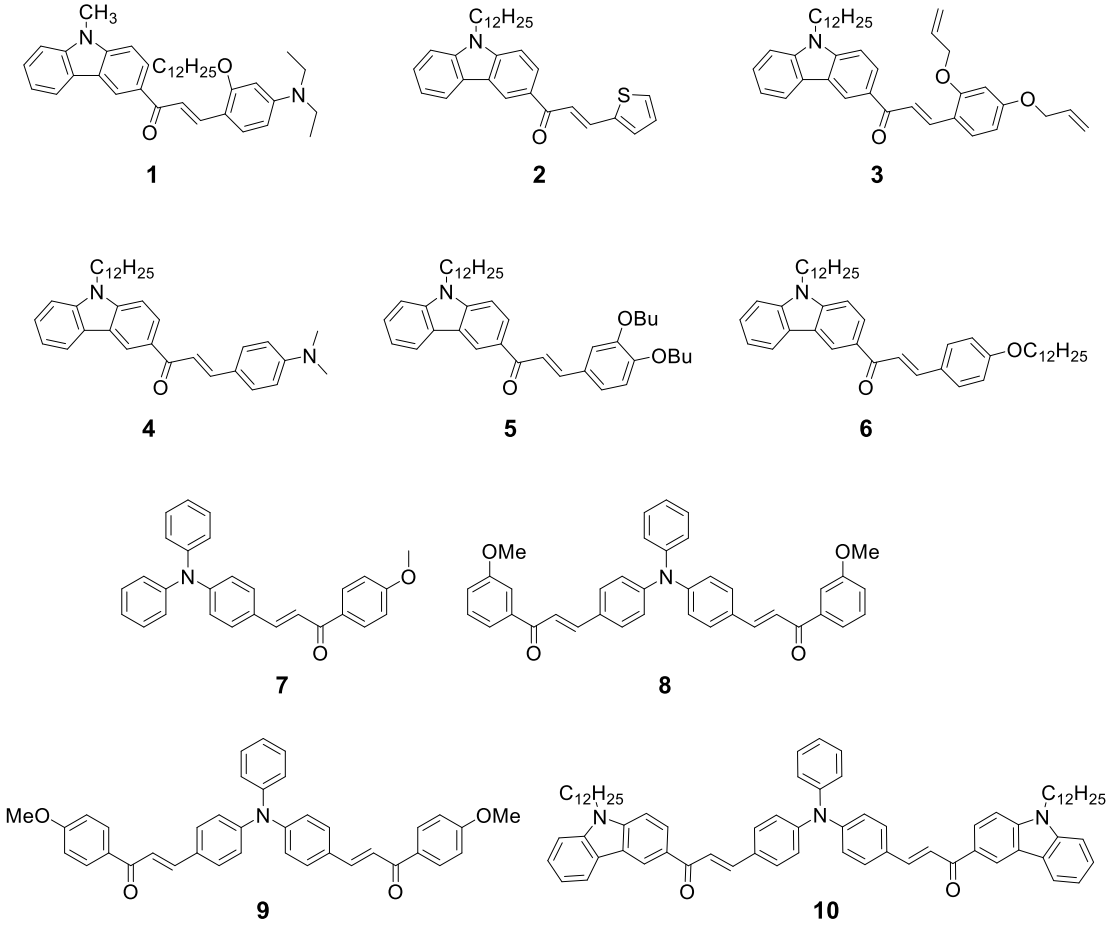

Scheme1. Chemical structures of chalcones 1-10 examined in this study.

2. Materials and Methods

Materials：

The carbazole or triphenylamine (TPA)-based mono-chalcones used as photoinitiators were synthesized as reported in the supporting information, and the chemical structures are presented in the Scheme 1. The PEG-diacrylate: SR 610 was obtained from Sartomer-Europe and used as the monomer for the free radical photopolymerization. Phenyl-N-*tert*-butylnitrone (PBN) was purchased from Sigma-Aldrich (St. Louis, MO, USA). *Bis*-(4-*tert*-butylphenyl) iodonium hexafluorophosphate (iodonium salt, Speedcure 938) and ethyl 4-dimethylaminobenzoate (amine, Speedcure EDB) were all

purchased from Lambson (Lambson Ltd., Wetherby, UK) and used as co-initiator and electron donor, respectively. Corresponding molecular structures are shown in Scheme 2. All solvents used in this work were of analytical grade and purchased from Sigma-Aldrich (St. Louis, MO, USA).

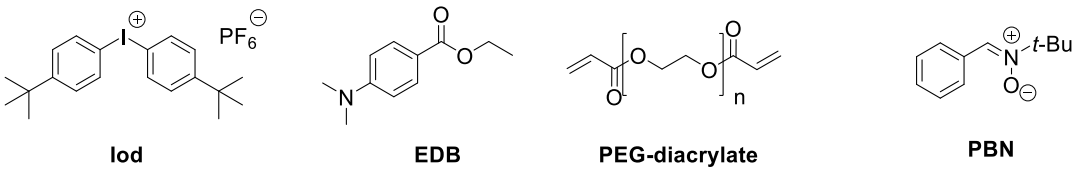

Scheme 2. Chemical structures of other compounds used in this study.

Free Radical Photopolymerization Experiments: In order to study the influence of the chalcones/Iod/amine, chalcones/Iod and chalcones/amine combinations as well as chalcones alone on the photopolymerization efficiency, the weight percent of chalcones, iodonium salt and amine were optimized separately and the best conditions were the following ones (chalcones/Iod/amine: 1.5%/1.5%/1.5%, w/w/w in PEG-diacrylate) for our experiments. Photosensitive formulations were polymerized between two polypropylene (PP) films with 1 drop of resin sandwiched between the two films to reduce the O_2 inhibition or into molds (under air) for thick samples. The different samples were polymerized upon irradiation with a LED @405 nm at room temperature. To evidence the crucial role of the chalcone in these formulations, the Iod/amine (1.5%:1.5%, w/w) based two-compound PIS was used as a blank control. An excellent solubility of all systems was observed in PEG-diacrylate monomers. The decrease of the double bond content of (meth)acrylate functions were continuously monitored by real time (RT) FTIR spectroscopy (JASCO FTIR 4100, Oklahoma City, OK, USA). Evolution of the methacrylate characteristic peaks was followed by FTIR in the near infrared range at ~ 6160 cm^{-1} for the thick samples and at ~1600 cm^{-1} for the thin films. The procedure used to monitor the photopolymerization profiles has been already described in detail in a previous report [46].

UV-Visible Absorption Experiments : The UV-visible absorption properties of different chalcones dissolved in acetonitrile at a concentration of 1 * 10^{-5} M were studied using JASCO V730 spectrophotometer. Furthermore, photolysis of these PISs was investigated under LED@405 nm where the concentration of chalcones was 5 × 10^{-5} M, the concentration of iodonium salt (Iod) and amine was 0.01 M.

Fluorescence and Cyclic Voltammetry Experiments: Fluorescence properties of the different chalcones dissolved in acetonitrile at a concentration of 1 * 10^{-5} M were studied using JASCO FP-6200 spectrofluorimeter. In addition, the fluorescence quenching experiments of the chalcones by Iod or amine were carried out in acetonitrile.

The redox potentials (oxidation potential E_{ox} vs. SCE and reduction potential E_{red} vs. SCE) for the different chalcones were measured in acetonitrile by cyclic voltammetry with tetrabutylammonium hexafluorophosphate (Aldrich) 0.1 M as the supporting electrolyte. A platinum electrode was used as a working electrode and a saturated calomel electrode (SCE) was used as a reference electrode. Moreover, the free energy change $\Delta G^{S1}{}_{Iod}$ or $\Delta G^{S1}{}_{EDB}$ for an electron transfer reaction from the singlet state were calculated from equation 1 or 2 (eq. 1 or 2) where E_{ox}, E_{red} and E_{S1} are the oxidation potential of the electron donor, the reduction potential of the electron acceptor and the excited state energy level (determined from the UV-visible and fluorescence experiments), respectively. Similarly, the free energy change of the triplet state $\Delta G^{T1}{}_{Iod}$ or $\Delta G^{T1}{}_{EDB}$ was calculated from equations 3 and 4 (eq. 3, eq. 4) where E_{T1} is the triplet state energy level (determined from molecular modeling). The reduction potential of the iodonium salt was -0.7 V and the oxidation potential of EDB was 1.0 V according to literature data [47].

$$\Delta G^{S1}{}_{Iod} = E_{ox} - (-0.7) - E_{S1} \quad (1)$$

$$\Delta G^{S1}{}_{EDB} = 1 - E_{red} - E_{S1} \quad (2)$$

$$\Delta G^{T1}{}_{Iod} = E_{ox} - (-0.7) - E_{T1} \quad (3)$$

$$\Delta G^{T1}{}_{EDB} = 1 - E_{red} - E_{T1} \quad (4)$$

Electron Spin Resonance-Spin Trapping (ESR-ST) Experiments: The ESR-ST experiments were carried out using an X-band spectrometer (EMX plus, Bruker). LED@405 nm was used as the irradiation source for trapping the production of radicals at room temperature in N_2 saturated *tert*-butylbenzene solutions and trapped by phenyl-*N*-*tert*-butylnitrone (PBN) according to the procedure described in detail. ESR spectra simulations were carried out using WINSIM software [48].

3D Printing Experiments: A computer programmed laser diode @405nm (Thorlabs) with a spot size of about 50 μm was used as the light source to produce specific three-dimensional patterns from the developed two-component PISs with PEG-diacrylate. Photosensitive formulations were polymerized under air in a homemade glass square tank (2mm thickness) and the generated patterns were analyzed by a numerical optical microscope (DSX-HRSU from Olympus Corporation, Tokyo, Japan); different laser speeds were investigated.

Swelling Experiments: The swelling of PEG polymerized by the two-component PISs based on chalcones/Iod (1.5%/1.5%, w/w) were measured by immersing the polymerization products in deionized water at room temperature, and then removing them (n = 4) after 24h, blotting the residual water on the surface of the products quickly with paper. After that, the wet weight of each polymerization product (Wt) was measured and compared with the initial wet weight (Wo). The swelling ratio (Sr) was defined by equation 5 [49], as follows:

$$\mathbf{Sr\ (\%) = (Wt\text{-}Wo)/Wo \times 100} \qquad \mathbf{(5)}$$

4D Printing Experiments: The reversible deformation effect of the PEG based polymers prepared with the two-component PISs based on chalcones/Iod (1.5%/1.5%, w/w) upon irradiation with LED@405nm for 1 min were measured via swelling and dehydration stimuli: first immersing the polymerization products in water at room

temperature for 1 min; and then removing them @100 ^{o}C for 12 min; finally, removing the products @room temperature.

Molecular Modeling: Molecular orbital calculations were carried out with the Gaussian 03 suite of programs. The electronic absorption spectra for the 10 different carbazole or TPA-based mono-chalcones were calculated with the time-dependent density functional theory at the MPW1PW91/6-31G* on the relaxation geometries calculated at UB3LYP/6-31G* theory level.

3. Results and Discussion

3.1. Synthesis of Chalcones 1-10.

Chalcones are an important class of natural compounds exhibiting a variety of biological activities [25] so that the access to natural and non-natural structures has been the purpose of numerous researches. Accompanying this need, development of new synthetic methodologies to prepare chalcones has been extensively studied [50]. All chalcones presented in this study have been synthesized by a Claisen-Schmidt reaction between aldehydes **A1-A8** and aromatic ketones **K1-K4** under basic conditions [45]. Thus, by using an aqueous KOH solution and by performing the reactions in ethanol, the different chalcones **1-10** could be prepared with reaction yields ranging from 45% for chalcone 8 and 87% for chalcone 4 (See Figure 1). All chalcones were obtained as solids and their chemical structures were investigated by ^{1}H, ^{13}C NMR, and HRMS spectroscopies (see Supporting Information).

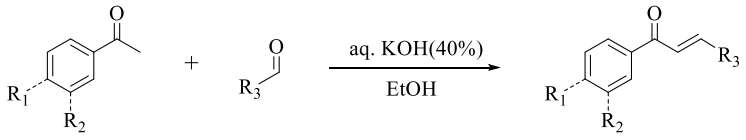

K1-K3 **A1-A7**

Chalcone 1 (K1, A1): 78% yield; **Chalcone 2 (K2, A2):** 86% yield
Chalcone 3 (K2, A3): 79% yield; **Chalcone 4 (K2, A4):** 87% yield
Chalcone 5 (K2, A5): 80% yield; **Chalcone 6(K2, A6):** 82% yield
Chalcone 7 (K3, A7): 64% yield

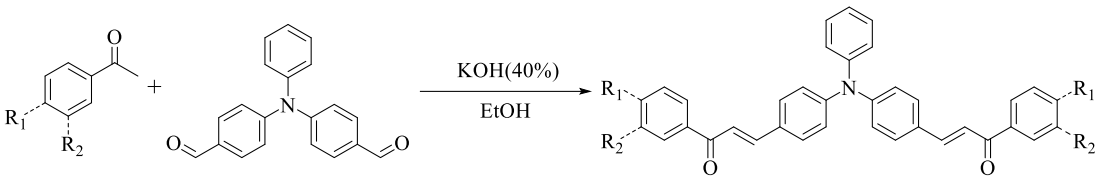

K2-K4 **A8**

Chalcone 8 (K4, A8): 45% yield;
Chalcone 9 (K3, A8): 51% yield
Chalcone 10 (K2, A8): 57% yield

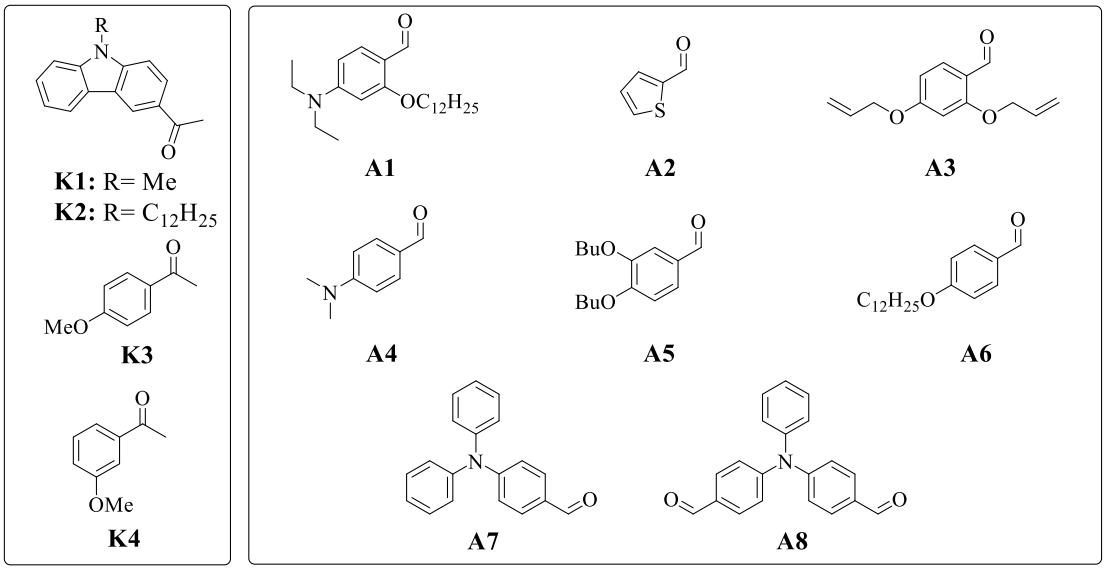

Figure 1. Synthetic routes to chalcones 1-10.

3.2. Photoinitiation Ability of the Chalcones based PISs.

In order to study the ability of chalcones to act as photoinitiators with additives (Iod and EDB), Real-Time Fourier Transform InfraRed (RT-FTIR) technique was used to monitor the associated polymerization profiles upon irradiation with a LED@405 nm. Four different photoinitiating systems were investigated: i) chalcone/Iod/amine (1.5%/1.5%/1.5%, w/w/w) three-component PIS, ii) chalcone / Iod (1.5%/1.5%, w/w) and chalcone/EDB (1.5%/1.5%, w/w) two-component PIS and

iii) chalcones aloneas PI (1.5% w/w) to initiate the free radical polymerization of PEG-acrylate monomers both in thin films and thick films.

Under the same irradiation conditions, the samples containing only chalcones were not polymerized either in thick molds or thin films (See Figure S1b). After addition of EDB, the samples could be polymerized between thin films under LED@405nm, while all of them still weren't polymerized in thick molds (See Figure S1a), which indicates that EDB can improve the polymerization efficiency when combined with chalcones. Furthermore, samples based on the two-component chalcones/Iod PISs and the three-component chalcones/Iod/amine PISs would be polymerized efficiently both in the thick molds and thin films. In addition, the efficiencies of these two latter systems (chalcone/Iod and Chalcone/Iod/EDB) are better than the other two systems (Chalcone alone or Chalcone/EDB). Typical acrylate function conversions vs irradiation time profiles are shown in Figure 2, and the corresponding final acrylate function conversion (FC) are outlined in Table 1, respectively.

As shown in Figure 2a, the polymerization profiles of all the three-compound PISs are much better than the blank control which is only composed of the co-initiators (Iod, 1.5%, w/w and amine, 1.5%, w/w), thus demonstrating the huge effect of the presence of the carbazole/TPA-based chalcones (See Figure 2a). Furthermore, by comparing Figures 2a and 2c, it's clear that the polymerization efficiency of the combination of chalcone / Iod (1.5% / 1.5%, w / w) is better than that of the three-component systems, which may be due to the fact that EDB competes with the electron-donating group inside the structure of chalcones to reduce the polymerization efficiency of the three-component PIS. Nevertheless, in comparison with the effectiveness of the final monomer conversions (in the Table 1) and the rates of the polymerization reaction (the slope of the curves), much better efficiencies were achieved when using the chalcone 4 and 10 based two-component PISs (e.g., FCs are 94% and 93%, respectively).

In the Figure 2b, RT-FTIR monitoring of the polymerization process for the 10 different chalcones in thick molds was extended until 600 s due to the lower efficiency of the three-component systems in these thick sample conditions. Indeed, compared to the blank control which is capable to furnish a FC of 93%, all the three-component systems furnished a lower final monomer conversion except the system based on chalcone 7 which provided a final conversion on par with that of the

reference system (FC = 92%) and a higher polymerization rate. In addition, according to the Figure 2d, it's obvious that the polymerization profiles of these two-compound PISs based on chalcone / Iod are much better than that of the three-component systems except for chalcones 1, 2 and 8, which further prove that EDB can inhibit the generation of free radicals and reduce the efficiency of the free radical polymerization of PEG-acrylate monomers when combined with Iod and chalcones. Remarkably, the polymerization efficiency is straightforwardly related to the absorption properties of the chalcone derivatives as chalcones 4 and 7 were the leaders in the efficiency trend and also exhibit the higher extinction coefficients at 405 nm, outperforming the others (see Table 2).

More interestingly, the chalcone 7 based three-component PIS (chalcone/Iod/amine) and two-component PIS (chalcone/Iod) were able to induce the polymerization of PEG-acrylate monomers automatically in several minutes upon daylight without light irradiation in thick molds showing a huge photosensitivity; while this phenomenon does not occur in the presence of chalcone 7/EDB based PIS or chalcone 7 based PI. In addition, all chalcones showed a yellow fluorescence during the photopolymerization process and the color of the polymers obtained after polymerization were clearly deepened or even changed to red or purple [51]. As chalcones 4, 7 and 10 demonstrated the highest efficiency for the thick molds and thin samples both in the combination with Iod or Iod/EDB, they were selected from the series of 10 chalcones for the following chemical mechanism investigation.

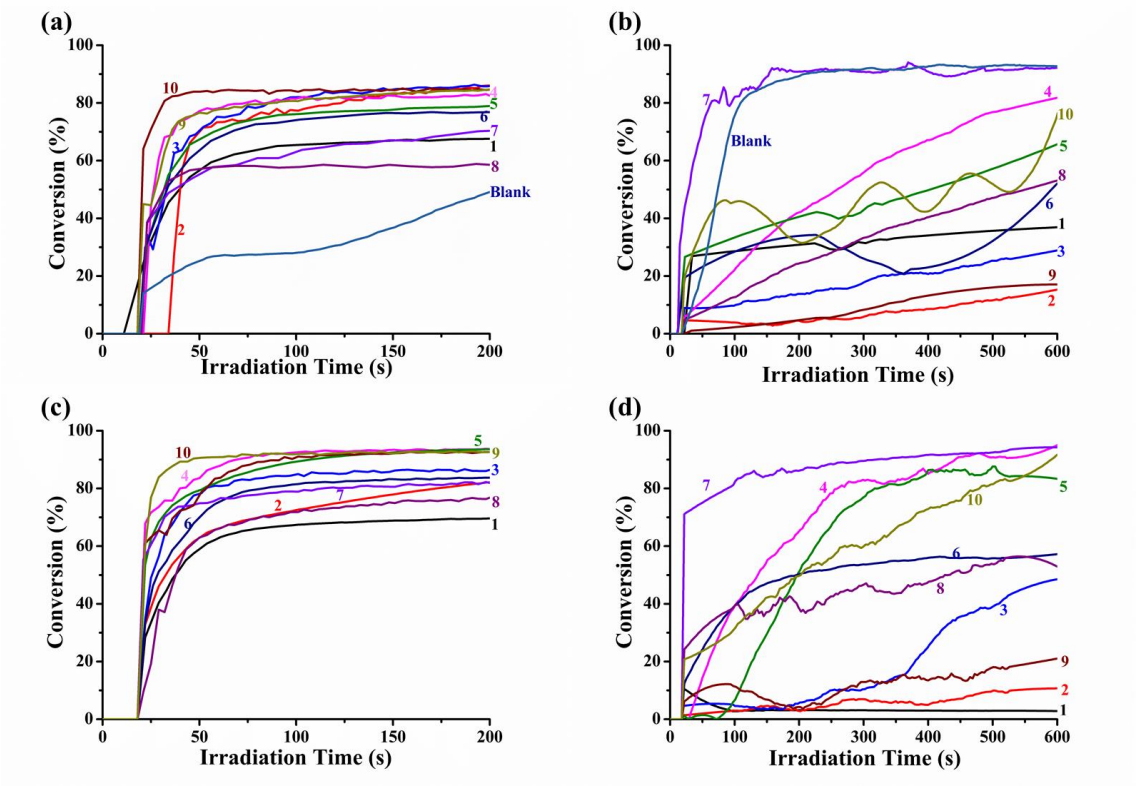

Figure 2. Photopolymerization profiles of PEG-diacrylate (acrylate function conversion vs irradiation time) upon exposure to a LED@405nm in laminate, in the presence of chalcones 1-10, (a) in thin films in presence of the iodonium salt (Speedcure 938) and amine (Speedcure EDB); (b) in thick molds in presence of the iodonium salt (Speedcure 938) and amine (Speedcure EDB), (c) in thin films in presence of the iodonium salt (Speedcure 938); (d) in thick molds in presence of the iodonium salt (Speedcure 938), at the same weight ratio chalcones 1-10: Iod: EDB=1.5%:1.5%:1.5% in 1g PEG, the irradiation starts for t = 20 s.

Table 1. Summary of the final acrylate function conversion (FCs) obtained for the PEG-diacrylate monomer while using the three-component PISs based on chalcones (1.5%, w/w)/Iod (1.5%, w/w)/amine (EDB, 1.5%, w/w) and using the two-component PISs based on chalcones (1.5%, w/w)/Iod (1.5%, w/w) both in thin films and in thick molds upon LED@405nm exposure in laminate.

Chalcone initiating systems in PEG-diacrylate				
chalcones	**chalcone/Iod/EDB**		**chalcone/ Iod**	
	Thin films	**Thick molds**	**Thin films**	**Thick molds**
1	68%	37%	70%	3%
2	86%	15.4	82%	11%
3	86%	29%	87%	49%

4	82%	82%	94%	95%
5	79%	66%	94%	84%
6	77%	52%	84%	57%
7	71%	92%	82%	94%
8	58%	53%	77%	52%
9	85%	17%	93%	21%
10	85%	77%	93%	92%
Blank	50%	93%		

3.3 Proposed Chemical Mechanisms

3.3.1 UV-Visible Absorption Properties of the Chalcones in Acetonitrile

The ground state absorption spectra of the novel photoinitiators (chalcones 1-10) in acetonitrile are shown in Figure 3, and the related parameters are presented in the Table 2. Except the four compounds chalcones 2, 3, 5 and 6 which exhibit high extinction coefficients around 360 nm, all the other compounds exhibit high extinction coefficients (ε_{max}) in the visible range (e.g., 23900 $M^{-1}cm^{-1}$ for chalcone 4, 18740 $M^{-1}cm^{-1}$ for chalcone 7 and 9020 $M^{-1}cm^{-1}$ for chalcone 10). The maximum absorption of chalcones 4, 7 and 10 appeared around 408 nm, 405nm and 430 nm, guaranteeing a good overlap with the emission spectrum of the LED@405 nm used in this work.

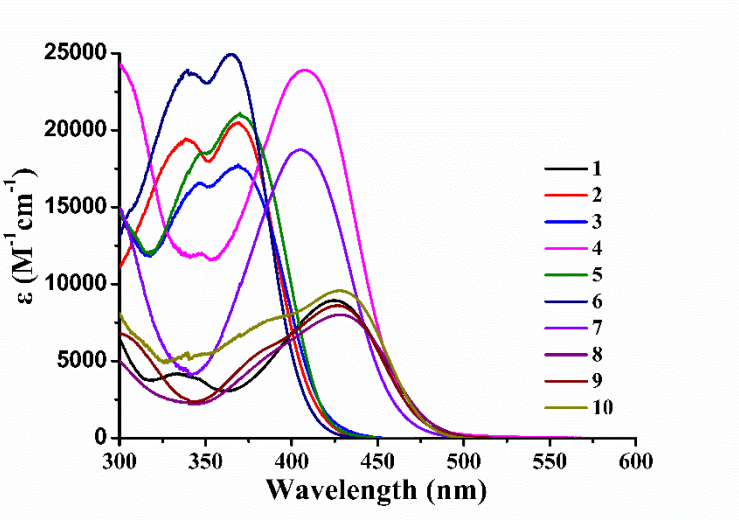

Figure 3. The UV-visible absorption spectra of chalcones 1-10 in acetonitrile.

Table 2. Light absorption properties of chalcones in acetonitrile: maximum absorption wavelengths λ_{max}; extinction coefficients at λ_{max} (ε_{max}) and extinction coefficients at the emission wavelength of the LED@405 nm ($\varepsilon_{@405nm}$).

	λ_{max} (nm)	ε_{max} ($M^{-1} cm^{-1}$)	$\varepsilon_{@405nm}$ ($M^{-1} cm^{-1}$)
chalcone 1	425	8930	7450
chalcone 2	369	20520	4830
chalcone 3	369	17740	5960
chalcone 4	408	23900	23850
chalcone 5	370	21100	7020
chalcone 6	360	24900	3530
chalcone 7	405	18740	18740
chalcone 8	430	7990	6760
chalcone 9	428	8540	7200
chalcone 10	430	10500	9020

3.3.2. Steady State Photolysis of Chalcones Characterized by UV-Vis Spectroscopy

The steady-state photolysis experiments of chalcones 4, 7 and 10 in the presence of an iodonium salt and an amine in acetonitrile have been carried out. Upon irradiation with a LED@405 nm, obvious and significant declines of the UV-visible absorption intensity were observed (Figure 4). Photolysis of chalcone 4 was so fast that it completely decomposed within 9 s, and then, the second is chalcone 7 that completely decomposed within 36 s, while for chalcone 10, the photolysis was relatively slower, with a complete decomposition after 180 s, owing to its lower extinction coefficients compared to that of chalcones 7 and 10 (see in Table 2)

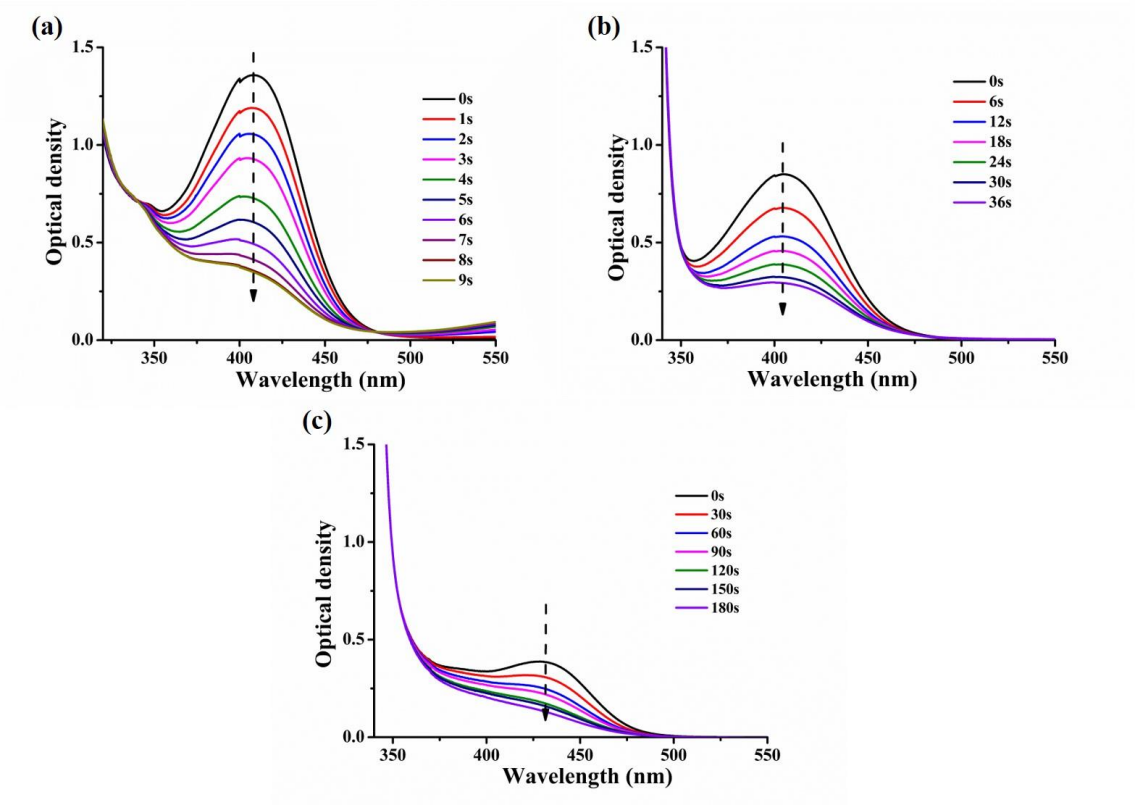

Figure 4. Steady state photolysis of chalcones (5×10^{-5} M in acetonitrile) in presence of the iodonium salt (Speedcure 938, 0.01M) and amine (Speedcure EDB, 0.01 M) upon exposure to a LED@405nm under air in the solvent of acetonitrile: (a) chalcone 4; (b) chalcone 7; (c) chalcone 10.

To better understand the interaction of the iodonium salt or the amine with the chalcones in the different systems, steady state photolysis of chalcones combined with the iodonium salt or the amine independently was also studied. As shown in Figure 5, in the presence of Iod, similar to previously mentioned for the three-component PIS, intensity of the characteristic peaks of chalcones in the UV-visible absorption spectra significantly decreased and were completely photolyzed in a short time under light irradiation. However, for the chalcone/amine systems (Figure S2), only the absorption spectrum of chalcone 4 decreased upon light irradiation even though it's very slow, while for chalcones 7 and 10, the absorption spectra did not change for the same irradiation time, which may be due to the introduction of an electron donating group - a carbazole or a methoxyphenyl group into the electron-withdrawing group of chalcones reducing the reaction efficiency between chalcones and EDB [40].

In addition, upon the light irradiation, the absorption spectra of chalcone 4 itself decreased slowly which was similar to the chalcone 4 / amine system, while for chalcones 7 and 10, like the chalcone / amine system, their absorption peaks did not change with the light irradiation (Figure S3). The above results indicate that an intramolecular charge transfer (ICT) can occur within the chalcone backbone and that chalcones can be combined with EDB to induce a reduction reaction (amine is electron donor), but all these reactions are poor and slow compared to the chalcone/Iod interaction.

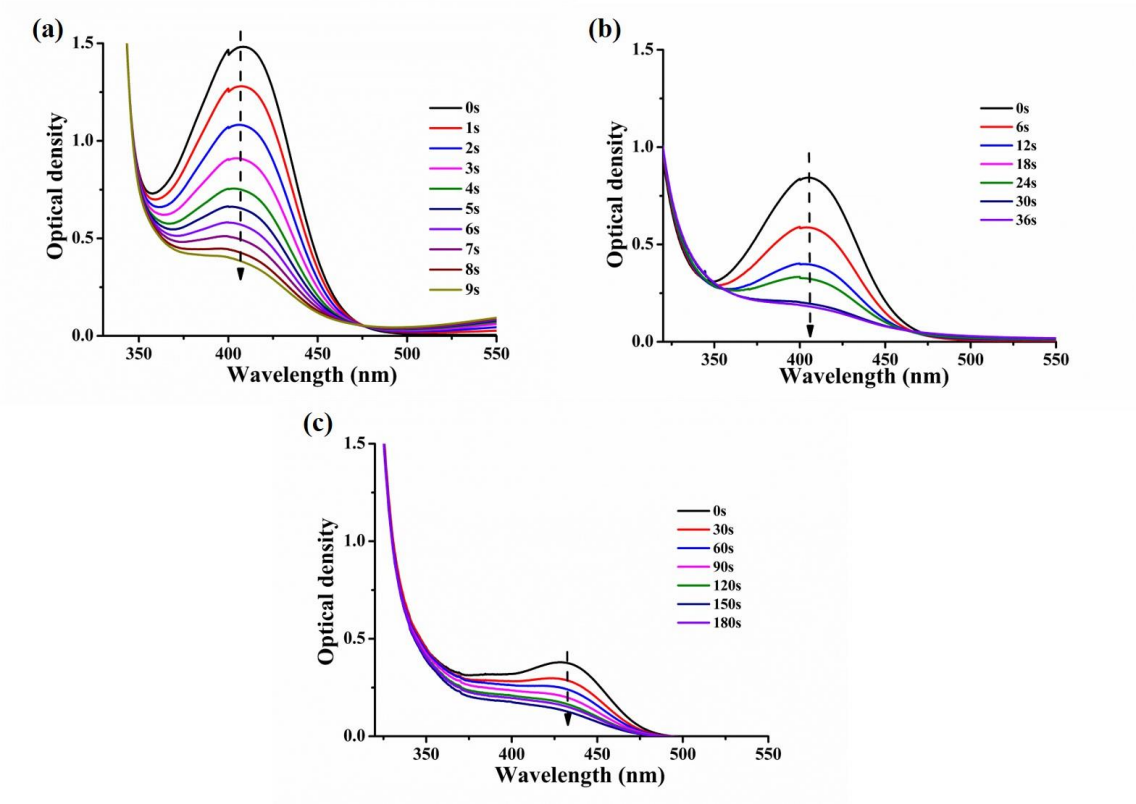

Figure 5. Photolysis of chalcones (5×10^{-5} M in acetonitrile) only in the presence of iodonium salt (Speedcure 938, 0.01M) upon exposure to a LED@405nm under air in the solvent of acetonitrile: (a) chalcone 4; (b) chalcone 7; (c) chalcone 10.

3.3.3. Consumption of Chalcones in Photolysis Reactions

As shown in the Figure 6, a summary of the consumption of the chalcones vs. the irradiation time based on the abovementioned photolysis reactions (i.e. in different two and three-component systems) is provided. It is obvious that the highest consumption

of chalcones 7 and 10 is achieved by the chalcones/Iod combinations (e.g. the consumption of chalcone 7 = 78% for chalcone 7/Iod, the consumption of chalcone 10 = 64% for chalcone 10/Iod), then, followed by that of the three-component PISs (chalcones/iodonium/amine) (e.g. 65% for chalcone7/Iod/amine and 55% for chalcone10/Iod/amine). However, for the same irradiation time, there were almost no consumption of chalcones 7 and 10 when using the two-component PISs based on chalcone 7/amine and chalcone 10/amine or the PI based on chalcones 7 and 10 itself due to the weak interaction between chalcones and EDB as well as the weaker electron transfer within themselves. It is thus proposed that the two reactions r1 and r2 (shown in the Scheme 3) occurred for the chalcones 7 and 10/Iod based two-component PIS as well as for the chalcones 7 and 10/Iod/amine based three-component PIS during the photolysis process. According to the Figure 6a, the chalcone 4/Iod combination and the chalcone 4/Iod/EDB combination achieved the highest consumption of chalcone (~74%) together, while the chalcone 4/amine system led to the lowest consumption (~19%). Furthermore, the consumption of chalcone 4 itself (21%) is slightly higher than that of chalcone 4/amine system. EDB can be involved in (r3) but also in the regeneration of the chalcone through (r4). Chalcones can also be regenerated from chalcone-H$^{\bullet}$ in the presence of iodonium salt (r5).

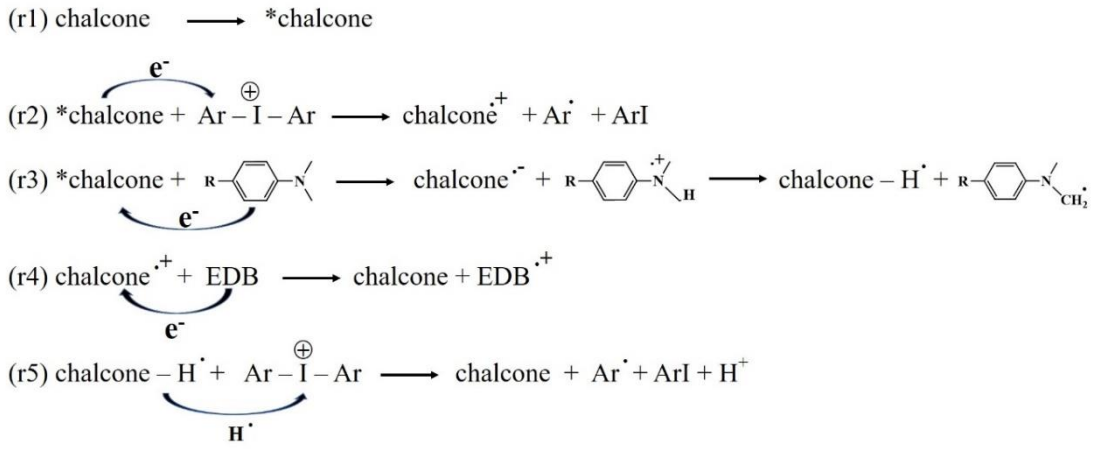

Scheme 3. Proposed mechanisms for the chalcones/Iod/amine initiating systems.

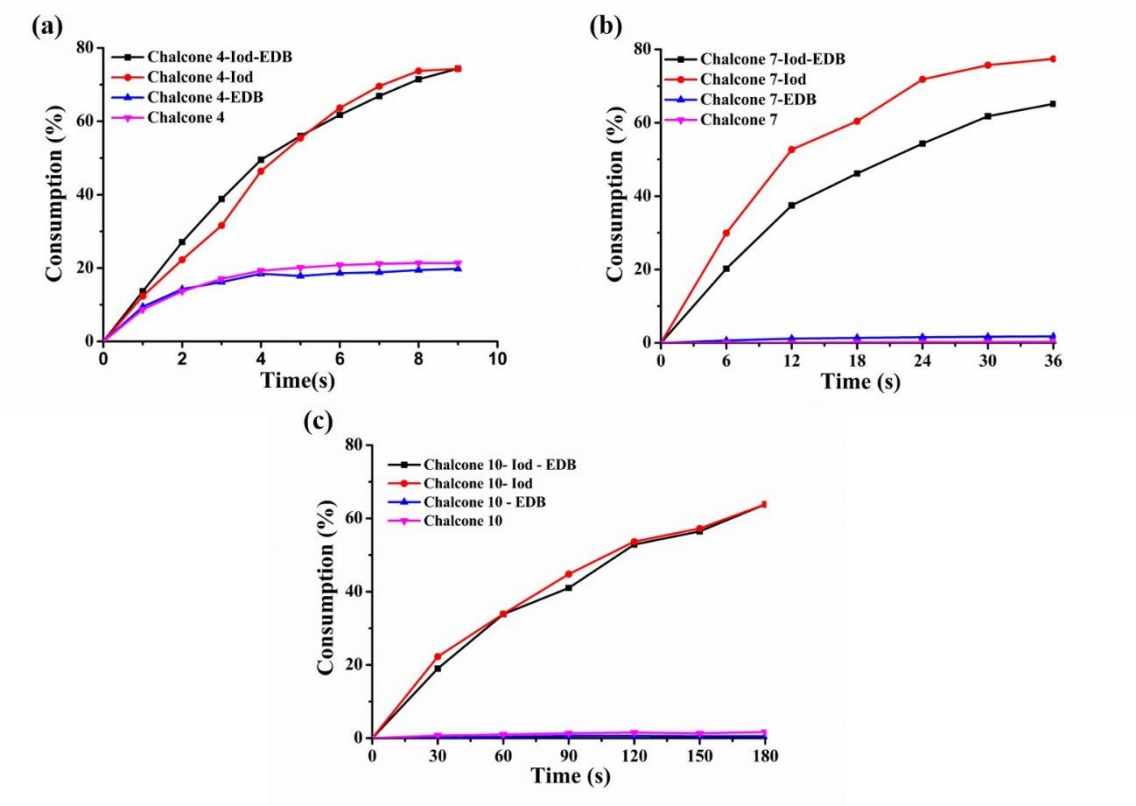

Figure 6. Consumption of (a) chalcone 4; (b) chalcone 7; (c) chalcone 10 during the photolysis experiments.

3.3.4 Fluorescence Quenching Experiments and Cyclic Voltammetry to Study Electron Transfer Reaction in Chalcone based systems

The first singlet excited state energy (E_{S1}) of chalcones 4, 7 and 10 can be determined by the crossing point between the UV-visible absorption and the fluorescence spectra in acetonitrile, the data are presented in the Figure 7 (e.g. E_{S1} = 2.66 eV for chalcone 4, E_{S1} = 2.60 eV for chalcone 7 and 2.56 eV for chalcone 10; Table 3).

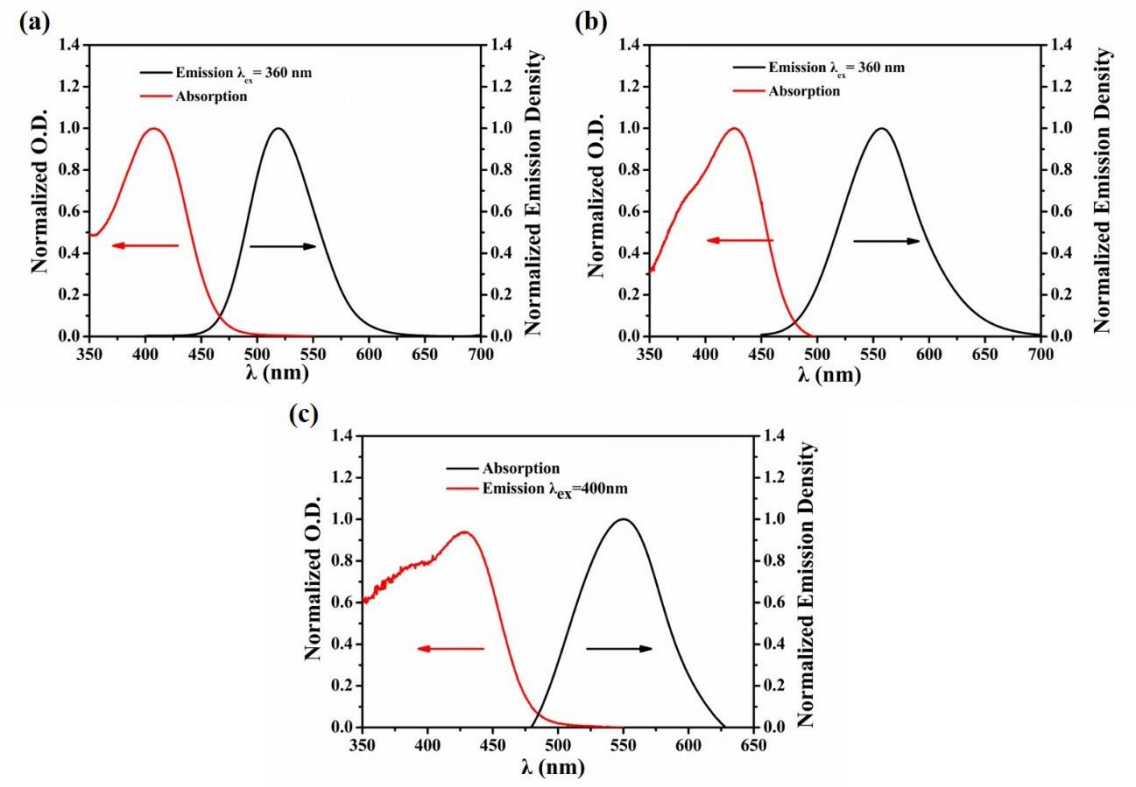

Figure 7. Singlet state energy determination in acetonitrile of (a) chalcone 4; (b) chalcone 7; (c) chalcone 10.

Fluorescence quenching experiments for chalcones 4, 7 and 10 have been conducted in acetonitrile to seek the theoretical feasibility of an electron transfer reaction with the iodonium salt (Iod) [52]. As shown in Figure 8, a linear fluorescence quenching with the addition of Iod were observed for chalcones 4, 7 and 10 in acetonitrile. Furthermore, favorable fluorescence quenching processes of the excited singlet states by Iod are shown by the high value of the Stern–Volmer coefficients (K_{SV}, Table 3) as well as the associated electron transfer quantum yield (ϕ_{et}, Table 3) for the expected electron transfer reaction between the chalcones and Iod (r2); ϕ_{et} were calculated applying the equation 6. Remarkably, very high electron transfer quantum yields (Φet) for chalcone 4 were calculated (Table 3) in agreement with efficient r2 and r3 processes. Compared to chalcone 4, chalcone 7 and 10 showed lower electron transfer quantum yields (ϕ_{et}), which can be probably attributed to a radiation-free excited state deactivation related to an aryl rings rotation [27,43].

$$\Phi^{et}{}_{Iod} = K^{sv}{}_{Iod} * [Iod] / (1 + K^{sv}{}_{Iod} * [Iod]) \quad (6)$$

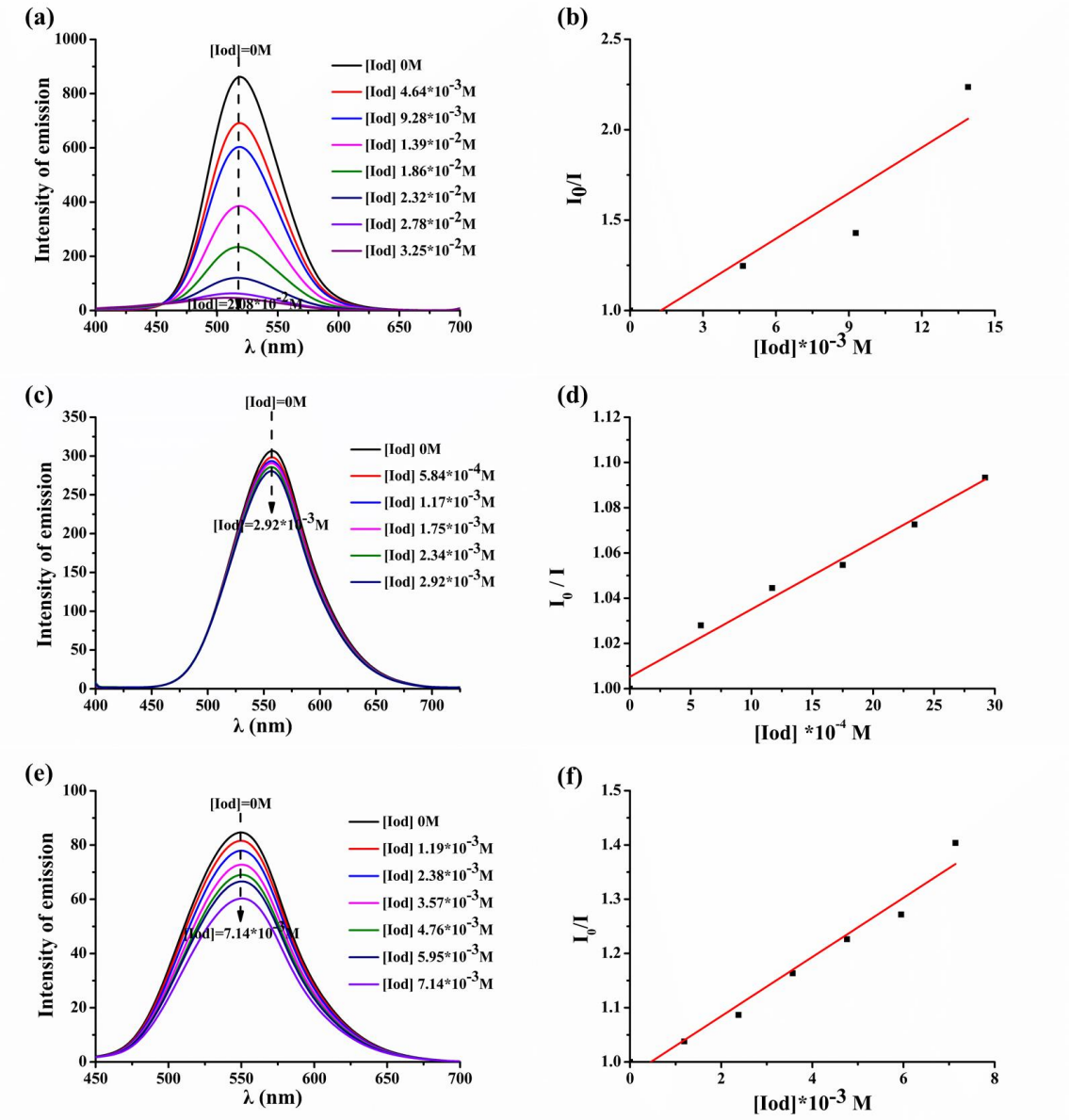

Figure 8. (a) Fluorescence quenching of chalcone 4 by iodonium salt (speedcure 938); (b) Stern-Volmer treatment for the chalcone 4/Iod fluorescence quenching; (c) Fluorescence quenching of chalcone 7 by iodonium salt (speedcure 938); (d) Stern-Volmer treatment for the chalcone 7/Iod salt fluorescence quenching. (e) Fluorescence quenching of chalcone 10 by iodonium salt (speedcure 938); (f) Stern-Volmer treatment for the chalcone 10/Iod salt fluorescence quenching.

For the mechanistic investigation, electrochemical reactions of chalcones 4, 7 and 10 were also examined by cyclic voltammetry. As shown in Figure 9, a favorable electron transfer reaction occurs in chalcone/Iod with negative free energy changes:

ΔG^{S1}_{Iod} = -1.73 eV, -1.41 eV and -1.53 eV for chalcones 4, 7 and 10, respectively (Table 3). Electron transfer reactions also occurred in chalcone / EDB (e.g., ΔG^{S1}_{EDB} = -0.98 eV, -1.12 eV and -1.5 eV for chalcones 4, 7 and 10 respectively, Table 3). Furthermore, for chalcone 10, two oxidation peaks were observed in the positive potential range, which can be related to a further oxidation (not reversible) event at higher potentials [43]. The obtained LUMO/HOMO energy levels (Highest Occupied Molecular Orbital HOMO and Lowest Unoccupied Molecular Orbital LUMO) are shown in Figure S4. The HOMO of chalcones 7 and 10 are located mainly over the TPA moiety. Concerning the LUMO, for chalcones 7 and 10, this orbital is centered over the enone and vinyl-substituted aryl groups. However, for chalcone 4, the HOMO and LUMO are mainly located over the enone and aryl substituted with dimethylamine moiety. Moreover, triplet state energy levels (E_{T1}) of chalcones were also simulated and the results are presented in Figure S4. By calculating the free energy change of triplet state ΔG^{T1} from equations 3 and 4, the reaction of triplet state of chalcones 4, 7 and 10 with iodonium salt and EDB are also favorable ($\Delta G^{T1}_{Iod} < 0$ and $\Delta G^{T1}_{EDB} < 0$ in Table 3) always in agreement with Scheme 3 for the proposed mechanisms.

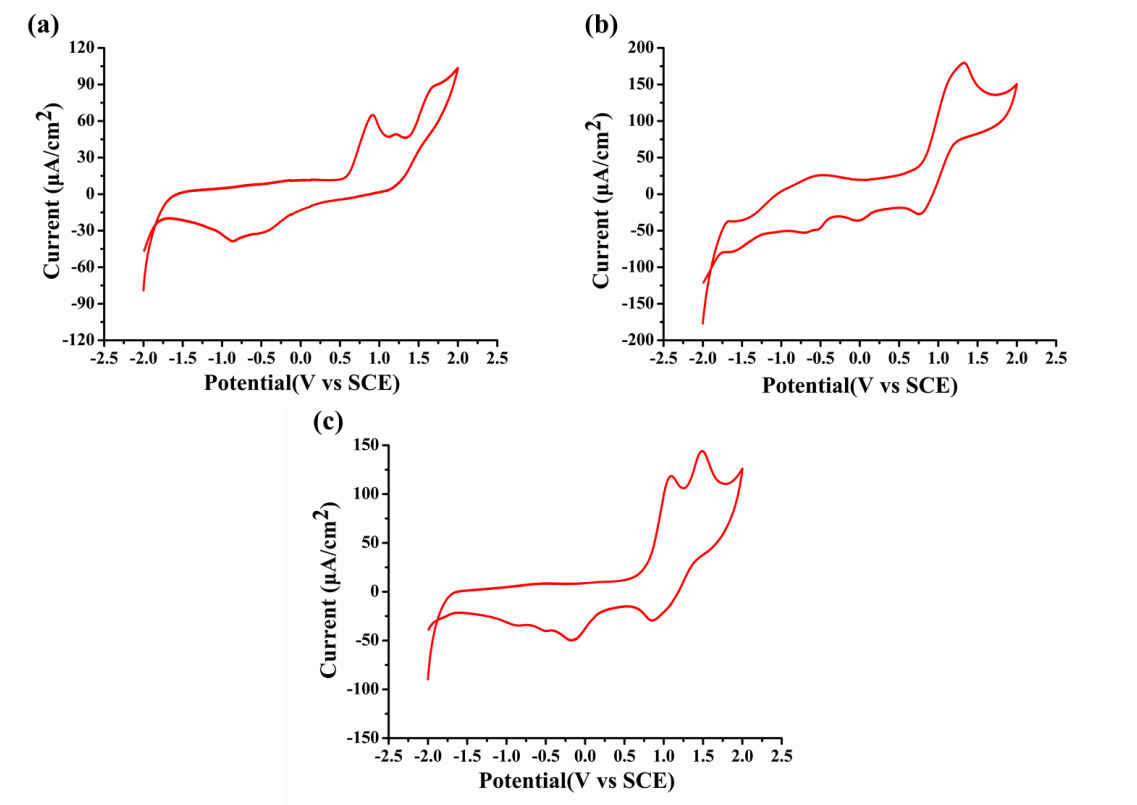

Figure 9. Cyclic voltammograms of chalcones 4, 7 and 10 in acetonitrile solvent against saturated calomel electrode (SCE) under a nitrogen saturated atmosphere. (a) chalcone 4; (b) chalcone 7; (c) chalcone 10.

Table 3. Parameters characterizing the fluorescence properties of chalcones 4, 7 and 10 in acetonitrile: Interaction rate constants (Ksv) of chalcone-Iod systems calculated by Stern-Volmer equation; electron transfer quantum yield (Φ^{et}_{Iod}) of chalcone/Iod interaction and singlet excited state energy (E_{S1}); oxidation potential (E_{ox}) and reduction potential (E_{red}) measured by cyclic voltammetry experiments as well as the parameters characterizing the chemical mechanisms associated with chalcones 4, 7 and 10 in acetonitrile.

	chalcone 4	**chalcone 7**	**chalcone 10**
K^{sv}_{Iod} (M^{-1})	240	29.9	54.8
Φ^{et}_{Iod}	0.88	0.48	0.63
E_{S1}（eV）	2.66	2.60	2.56
E_{T1}（eV）	2.12	2.05	2.05
E_{ox}（eV）	0.73	0.99	0.83

E_{red} (eV)	-0.68	-0.48	-0.06
ΔG^{S1}_{Iod}	-1.73	-1.41	-1.53
ΔG^{S1}_{EDB}	-0.98	-1.12	-1.5
ΔG^{T1}_{Iod}	-0.69	-0.86	-0.52
ΔG^{T1}_{EDB}	-0.44	-0.57	-0.99

3.3.5 ESR Experiments: free radicals generated in chalcone based systems

To better understand the interactions that took place in the different PISs, ESR-spin trapping (ESR-ST) experiments were carried out on chalcones 4, chalcone 4/Iod, chalcone 4/amine and chalcone 4/Iod/EDB solutions under N_2 in the presence of *N*-phenyl-*tert*-butyl nitrone (PBN) as the spin trap agent. As shown in the Figures 10a and b, in the presence of Iod and EDB, r2 and r3 occur: aryl radical and aminoalkyl radical adducts were clearly observed in ESR-ST [46, 52]. For the chalcone/Iod system (Figure 10 c and d), the PBN/aryl radical adduct is characterized by a_N = 14.4 G and a_H = 2.2 G [52], which is presently in full agreement with r2. While for the chalcone/EDB system (Figure S5 a and b), the hyperfine coupling constants for nitrogen and hydrogen were characterized by a_N = 14.4 G and a_H = 2.1 G that evidenced the generation of an aminoalkyl radical (r3) according to experimental data published elsewhere (a_N = 14.1 G and a_H = 2.1 G [46]). In addition, as shown in Figure S5 c and d, efficient intramolecular reactions occur in chalcones alone upon irradiation and radical adducts can also be observed (hyperfine coupling constants for nitrogen and hydrogen of a_N = 14.4 G and a_H = 2.2 G) in agreement with the photolysis of chalcones alone.

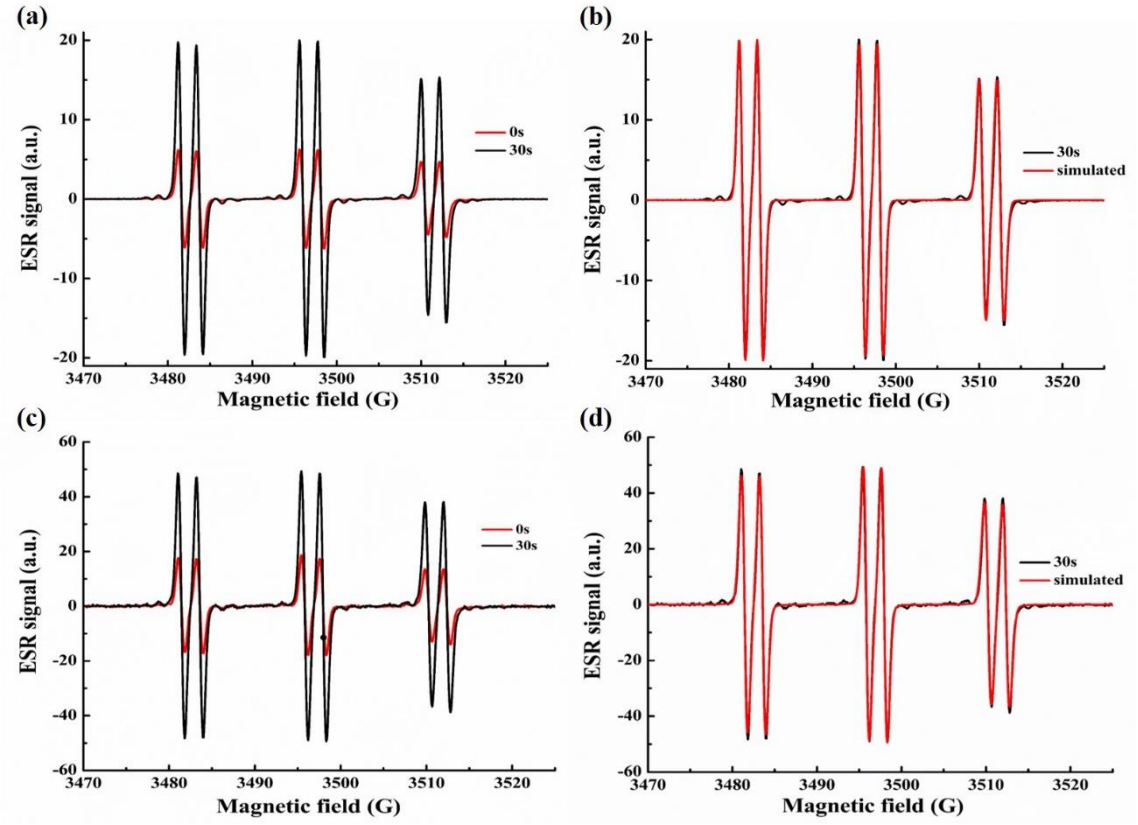

Figure 10. ESR spectra obtained from ESR-spin trapping experiment using PBN = 2 mg/mL (as spin trap agent); iodonium salt (Speedcure 938) = 12.6 mg/mL; amine (Speedcure EDB) = 12.6 mg/mL and chalcone 4 = 0.8 mg/mL in *tert*-butylbenzene under N_2. (a) chalcone 4/Iod/EDB Irradiation time = 0 s (red) and = 30 s (black) spectra; (b) chalcone 4/Iod/EDB Irradiation time = 30 s experimental (black) and simulated (red) spectra; (c) chalcone 4/Iod Irradiation time = 0 s (red) and = 30 s (black) spectra; (d) chalcone 4/Iod Irradiation time = 30 s experimental (black) and simulated (red) spectra.

3.4. 3D Printing Experiments based on the Two-Component PISs.

Using a laser diode @405 nm, laser write experiments were successfully carried out under air with the two-component PIS based on chalcones/Iod (1.5%/1.5%, w/w), which is very reactive for the free radical polymerization of PEG-diacrylate monomer. Remarkably, the high photosensitivity of chalcones 4, 7 and 10/Iod based PISs allowed the PEG-diacrylate monomer to be effectively polymerized in 3D structures to obtain a stable 3D patterns (“**C H E**”) with a high spatial resolution and for a very short irradiation time (t≦2 min) (See Figure 11).

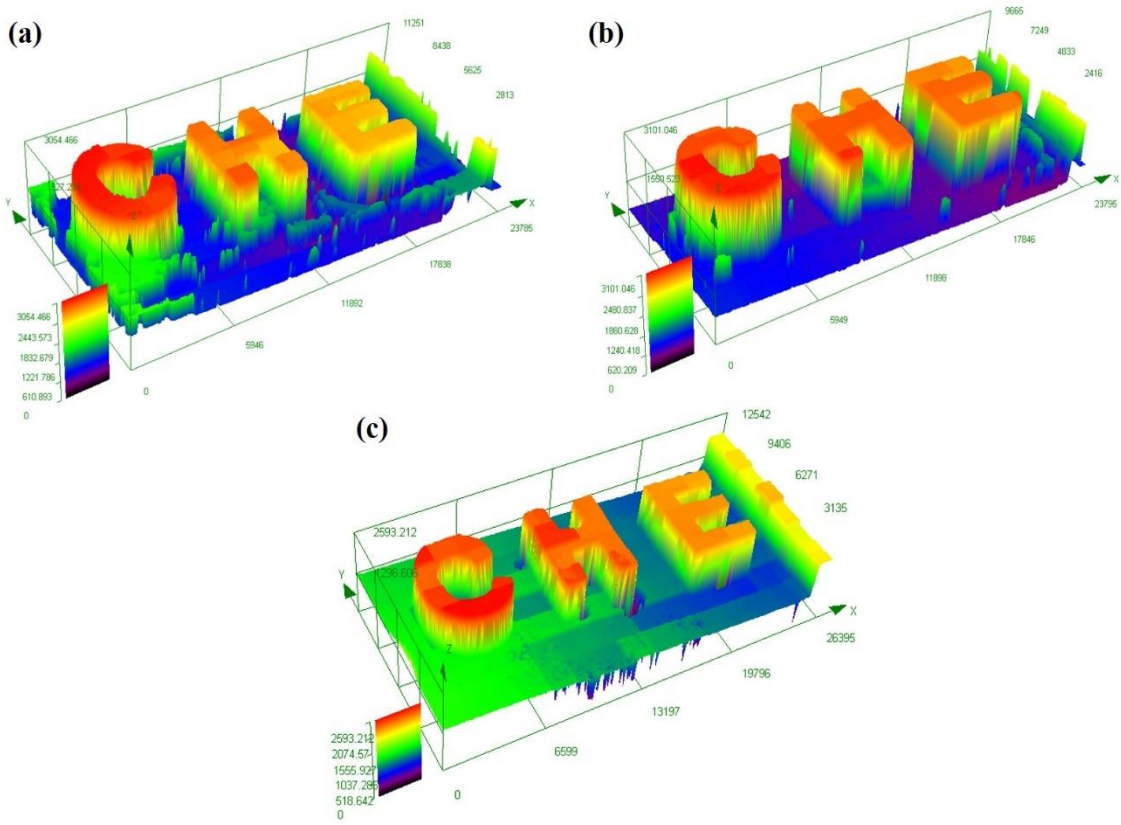

Figure 11. Free radical photopolymerization experiments for laser write of 3D patterns initiated by chalcones based two-component photoinitiating systems using PEG-diacrylate monomer. Characterization by numerical optical microscopy of the morphology of the 3D overall appearance of 3D patterns with chalcones/Iod (1.5%/1.5%, w/w) in PEG-diacrylate: (a) chalcone 4; (b) chalcone 7; (c) chalcone 10.

3.5. The Swelling of PEG-polymer Initiated by Chalcone/Iod

According to the Figure 12a, the swelling of the PEG-polymers obtained by photopolymerization using the two-component PIS based on chalcones/Iod (1.5%/1.5%, w/w) were investigated by immersing them into deionized water for 24 h. The best swelling ratio was obtained with chalcone 10 approaching 80%, then, followed by the products based on the chalcone 7 and chalcone 4, the swelling ratios of them were about 60%, which is due to the higher extinction coefficients at the emission wavelength of the LED@405 nm (e.g., 23850 $M^{-1}cm^{-1}$ for chalcone 4, 18740 $M^{-1}cm^{-1}$ for chalcone 7 and 9020 $M^{-1}cm^{-1}$ for chalcone 10), resulting in a higher degree of polymerization of chalcones 4 and 7. As shown in Figure 12b, the 3D patterns are also characterized by swelling properties. As a result of this, volumes of the different patterns increased by about 2-3 times (see Table 4) compared to that of their initial volumes. Furthermore, the different patterns could return to their primary appearance after heating during 3h at 50°C, enabling to remove the water contained in the

PEG-polymers, indicating that the swelling of these 3D patterns and polymers is reversible.

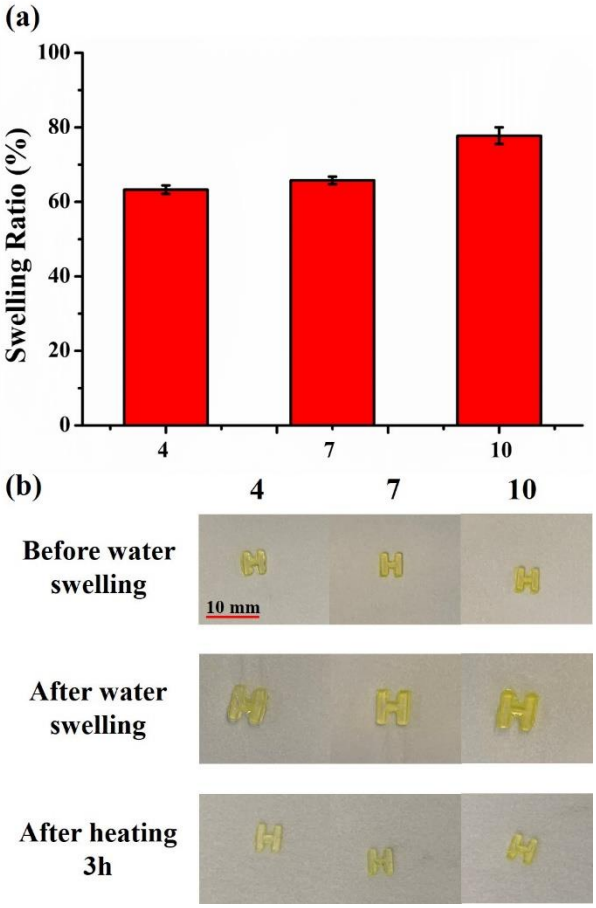

Figure 12. (a) the swelling ratio of PEG-polymer prepared using chalcones as photoinitiators; (b) the photos of the "H" 3D patterns based on PEG-polymers (obtained by laser write experiments using the chalcone/Iod two-component system) before water swelling, after water swelling for 24h and after heating for 3h to remove water.

Table 4. The volumes of the "H" 3D pattern in the cycle: without water (V_1), water swelling (V_2), water removal (V_3) as well as the increase rate of volume after swelling (R).

	chalcone 4	**chalcone 7**	**chalcone 10**
V_1 (mm^3)	12	12	12
V_2 (mm^3)	40.5	44.1	55.6
V_3 (mm^3)	12	12	12
R (%)	237.5%	267.5%	363.3%

3.6 Reversible Deformation: 4D behavior of PEG-polymer via Swelling and Dehydration Induced Actuation

Owing to the low solubility of typical photoinitiators in water, rather few aqueous 3D printing systems have been developed in literature [53-54]. Nevertheless, the newly proposed two-compound PIS in combination with PEG-diacrylate is suitable for 3D bioprinting with potential biocompatibility of aqueous systems. Apart from that, 4D printing products were manufactured using the proposed PIS through the swelling and dehydration induced actuation of the 3D printed hydrogels with spatial resolution characteristics. As the mechanical properties of PEG-diacrylate were dependent on the time of light exposure, different irradiation times were investigated to choose the best one. Specifically, a cross shaped object with spatially resolved properties was designed as shown in Figure 13 (a,b). After that, by placing the cross in a water filled beaker, we observed that it started to deform as swollen with water, resulting in a fully curled cross (namely, the degree change was approaching 180°) after swelling in water for 40s (Figure 13(c) and SI Video 1). Subsequently, the cross was removed from water and heated at 100^{o}C to induce evaporation. Correspondingly, the curled cross flattened and recovered to its original shape for 100s as the contained water removed (Figure 13(d) and SI Video 2). Then, by continuing to heat for 10 minutes as the cross completely dehydrated, it inverted curled as shown in Figure 13(e). Furthermore, we removed the cross from 100^{o}C to room temperature for 10 min, and the curled one could gradually flatten out or even return to its original shape (see Figure 13(f)). When we swelled the cross in the water again for 30 s, it could still deform completely again as shown in Figure 13(g) and SI Video 1. After heating at 100^{o}C for 100s, the curled cross restored to its original shape (see Figure 13(h) and SI Video 2). After continuous heating to complete dehydration, the cross reversed curl again (Figure 13(i)). These results demonstrated that the hydrogels initiated by the chalcone 7/Iod based novel PIS have a reversible deformation effect due to the thermal response and hydrophilic response [55-56].

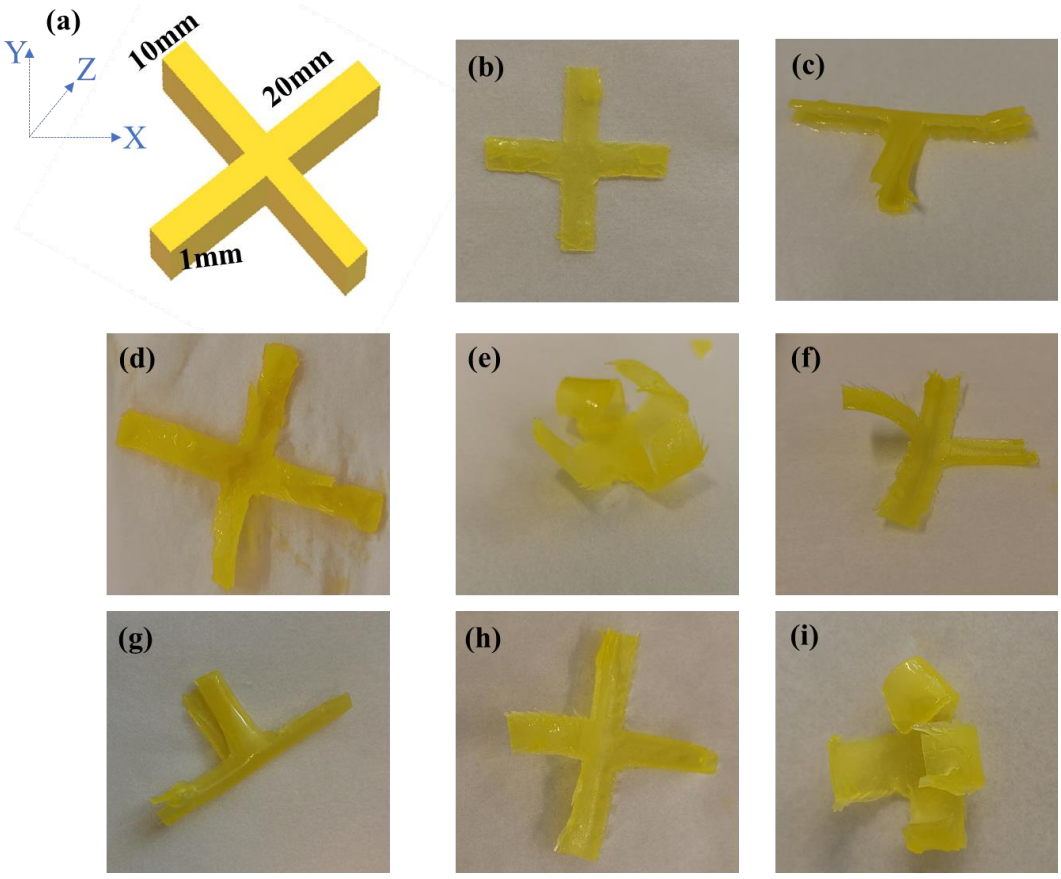

Figure 13. Swelling and dehydration induced actuation of PEG-polymers obtained using chalcone 7/Iod initiating system @405 nm. (a) the designed geometrical form of the cross; (b) cross of PEG-polymer after photopolymerization; (c) shape of the cross after water swelling for 1 min (see Video 1); (d) shape of the cross after 100 seconds of dehydration (heating at 100°C, see Video 1); (e) shape of the cross after 10 mins of dehydration (heating at 100°C); (f) cross after stay at room temperature for 10 mins; (g) shape of the cross after water swelling again for 1 min (see Video 2); (h) shape of the cross after 100 seconds of dehydration (heating at 100°C, see Video 2); (i) shape of the cross after 10 mins of dehydration (heating at 100°C).

4. Conclusions

In summary, a series of novel carbazole/TPA-based chalcones was synthesized and characterized. Remarkably, all chalcones presented in this work have never been reported in literature except chalcone 7 which was developed as the starting materials for the synthesis of novel pyrazolines used for optical materials [45]. All chalcones displayed a strong absorption in the visible range due to the introduction of the carbazole or the TPA chromophores, and these chalcones showed good efficiency for the free radical polymerization of acrylates under irradiation with a LED@405nm. Remarkably, chalcones 4, 7 and 10 proved to be excellent photoinitiators to boost

efficient kinetics for the polymerization of PEG-diacrylate while using iodonium salt as the electron-acceptor. Photoinitiation ability and the photochemical mechanisms of the new PISs have been studied by real-time Fourier Transform InfraRed (RT-FTIR) spectroscopy, fluorescence spectroscopy as well as ESR experiments. Finally, excellent 3D patterns with high resolution have been obtained by laser write experiments with the newly proposed three-component PISs. Apart from that, the shapes of 3D patterns can be reversibly modified by mean of a thermal response and a hydrophilic response of PEG for a 4D activation. Considering that the present work has clearly demonstrated the huge influence of the substitution pattern on the photoreactivity, future developments will consist in designing new carbazole and TPA-based chalcones to further improve their reactivity under the irradiation of longer-wavelength light.

Supplementary Materials:

The following are available online

Acknowledgments: Authors wish to thank the Region Grand Est (France) for the grant "MIPPI-4D". This research project is supported by China Scholarship Council (CSC) 201906280059. The DGA is acknowledged for its financial support through the PhD grant of Damien Brunel. This research was also funded by the Agence Nationale de la Recherche (ANR agency) through the PhD grant of Guillaume Noirbent (ANR-17-CE08-0054 VISICAT project). P. X. acknowledges funding from the Australian Research Council (FT170100301). This work was granted access to the HPC resources of the Mesocentre of the University of Strasbourg.

Conflicts of Interest:

The authors declare no conflict of interest.

References

1. T. Betancourt, J. Pardo, K. Soo, N.A. Peppas, Characterization of pH-responsive hydrogels of poly(itaconic acid-g-ethylene glycol) prepared by UV-initiated free radical polymerization as biomaterials for oral delivery of bioactive agents. *J. Biomed. Mater. Res. A* 2010, **93** (1), 175-88.
2. J.H. Lee, D.G. Bucknall, Swelling behavior and network structure of hydrogels synthesized using controlled UV-initiated free radical polymerization. *J. Polym. Sci. B Polym. Phys.* 2008, **46** (14), 1450-1462.
3. T. Watanabe, Y. Nishizawa, H. Minato, S. Chihong, K. Murata, D. Suzuki, Hydrophobic monomers recognize microenvironments in hydrogel microspheres during free radical seeded emulsion polymerization. *Angew. Chem. Int. Ed. Engl.* 2020, **59** (23), 8849-8853.
4. J. Ning, K. Kubota, G. Li, K. Haraguchi, Characteristics of zwitterionic sulfobetaine acrylamide polymer and the hydrogels prepared by free-radical polymerization and effects of physical and chemical crosslinks on the UCST. *Reactive and Functional Polymers* 2013, **73** (7), 969-978.
5. F. Marquardt, M. Bruns, H. Keul, Y. Yagci, M. Möller, Light-induced cross-linking and post-cross-linking modification of polyglycidol. *Chem. Commun*. 2018, **54**, 1647-1650.
6. E. Blasco, M. Wegener, C. Barner-Kowollik, Photochemically-Driven Polymeric Network Formation: Synthesis and Applications. *Adv. Mater*. 2017, **29**, 1604005.
7. S.C. Ligon-Auer, M. Schwentenwein, C. Gorsche, J. Stampfl, R. Liska, Toughening of photo-curable polymer networks: a review. *Polym. Chem*. 2016, **7**(2), 257-286.
8. N.S. Allen, Photochemistry and photophysics of polymer materials, Wiley, USA 2010.
9. D. Seliktar, Designing cell-compatible hydrogels for biomedical applications. *Science*, 2012, **336**(6085), 1124-1128.
10. H. Zhang, Molecularly imprinted nanoparticles for biomedical applications. *Adv. Mater*. 2020, **32** (3), e1806328.
11. J. Zhang, J. Lalevee, N.S. Hill, X. Peng, D. Zhu, J. Kiehl, F. Morlet-Savary, M.H. Stenzel, M.L. Coote, P. Xiao, Photoinitiation mechanism and ability of monoamino-substituted anthraquinone derivatives as cationic photoinitiators of polymerization under LEDs. *Macromol. Rapid. Commun*. 2019, **40(**16), e1900234.
12. J.-P. Fouassier, J. Lalevée, Photoinitiators for Polymer Synthesis-Scope, Reactivity, and Efficiency; Wiley-VCH Verlag GmbH & Co. KGaA: Weinheim, Germany, 2012.
13. P. Xiao, J. Zhang, F. Dumur, M.A. Tehfe, F. Morlet-Savary, B. Graff, D. Gigmes, J.-P. Fouassier, J. Lalevée, Photoinitiating systems: Recent progress in visible light

induced cationic and radical photopolymerization reactions under soft conditions. *Prog. Polym. Sci*. 2015, **41**, 32–66.
14. J.Z. Shao, Y. Huang, Q.G. Fan, Visible light initiating systems for photopolymerization: status, development and challenges. *Polym. Chem*. 2014, **5**, 4195–4210.
15. J.-P. Fouassier, X. Allonas, D. Burget, Photopolymerization reactions under visible lights: principle, mechanisms and examples of applications. *Prog. Org. Coat.* 2003, **47**, 16–36.
16. M.A. Tehfe, F. Dumur, P. Xiao, M. Delgove, B. Graff, J.-P. Fouassier, D. Gigmes, J. Lalevée, Chalcone derivatives as highly versatile photoinitiators for radical, cationic, thiol–ene and IPN polymerization reactions upon exposure to visible light. *Polym. Chem*., 2014, **5**, 382-390.
17. H. Chen, G. Noirbent, K. Sun, D. Brunel, D. Gigmes, F. Morlet-Savary, Y.J. Zhang, S.H. Liu, P. Xiao, F. Dumur, J. Lalevée, Photoinitiators derived from natural product scaffolds: mono-chalcones in three-component photoinitiating systems and their applications in 3D printing. *Polym. Chem*., 2020,**11**, 4647-4659.
18. B. Corakci, S.O. Hacioglu, L. Toppare, U. Bulut, Long wavelength photosensitizers in photoinitiated cationic polymerization: The effect of quinoxaline derivatives on photopolymerization. *Polymer* 2013, **54** (13), 3182-3187.
19. I. Gupta, P.E. Kesavan, Carbazole substituted BODIPYs. *Front. Chem*. 2019, **7**, 841.
20. N. Raghav, S. Jangra, M. Singh, R. Kaur, A. Rohilla, In-vitro studies of some chalcones on alkaline phosphatase. *Biochem. Pharmacol*.1991, **42**, 1447-1451.
21. R. Sónia, R. Daniela, F. Eduarda, F. Marisa, A systematic review on anti-diabetic properties of chalcones. *Curr. Med. Chem*. 2020, **27** (14), 2257-2321.
22. Y. Wang, W.D. Zhang, J.Q. Dong, J.B. Gao, Design, synthesis and bioactivity evaluation of coumarin-chalcone hybrids as potential anticancer agents. *Bioorg. Chem.* 2020, 103530.
23. M.B.Austin, J.P. Noel, The chalcone synthase superfamily of type III polyketide synthases. *Nat. Prod. Rep*., 2003, **20**, 79-110.
24. A. Boumendjel, J. Boccard, P.A. Carrupt, E. Nicolle, M. Blanc, A. Geze, L. Choisnard, D. Wouessidjewe, E.L. Matera, C. Dumontet, Antimitotic and antiproliferative activities of chalcones: forward structure–activity relationship. *J. Med. Chem*. 2008, **5**1(7), 2307-2310.
25. A. Rammohan, J.S. Reddy, G. Sravya, C.N. Rao, G.V. Zyryanov, Chalcone synthesis, properties and medicinal applications: a review. *Environ. Chem. Lett.* 2020, **18**, 433–458.
26. D.H. Choi, S.J. Oh, Photochemical reactions of a dimethacrylate compound containing a chalcone moiety in the main chain. *Eur. Polym. J*. 2002, **38**, 1559–1564.

27. K.I. Son, S.Y. Kang, D.Y.; Noh, Electrochemical and fluorescent properties of ferrocenyl-chalcone with N-Ethyl carbazole group. *Bull. Korean Chem. Soc*. 2009, **30**(2), 513-516.
28. F. Dumur, Carbazole-based polymers as hosts for solution-processed organic light-emitting diodes: simplicity, efficacy, *Org. Electron*. 2015, **25**, 345-361.
29. F. Dumur, L. Beouch, S. Peralta, G. Wantz, F. Goubard, D. Gigmes, Solution-processed blue phosphorescent OLEDs with carbazole-based polymeric host materials, *Org. Electron*. 2015, **25**, 21-30.
30. A. Al Mousawi, P. Garra, F. Dumur, T.T. Bui, F. Goubard, J. Toufaily, T. Hamieh, B. Graff, D. Gigmes, J.P. Fouassier, J. Lalevee, Novel Carbazole Skeleton-Based Photoinitiators for LED Polymerization and LED Projector 3D Printing. *Molecules* 2017, **22** (12), 2143.
31. B.P. Bandgar, L.K. Adsul, S.V. Lonikar, H.V. Chavan, S.N. Shringare, S.A. Patil, S.S. Jalde, B.A. Koti, N.A. Dhole, R.N. Gacche, A. Shirfule, Synthesis of novel carbazole chalcones as radical scavenger, antimicrobial and cancer chemopreventive agents. *J. Enzyme Inhib. Med. Chem.* 2013, **28** (3), 593-600.
32. M. Abdallah, D. Magaldi, A. Hijazi, B. Graff, F. Dumur, J.-P. Fouassier, T.T. Bui, F. Goubard, J. Lalevée, Development of new high performance visible light photoinitiators based on carbazole scaffold and their applications in 3D printing and photocomposite synthesis, *J. Polym. Sci. A Polym. Chem*. 2019, **57**, 2081-2092.
33. F. Dumur, Recent advances on carbazole-based photoinitiators of polymerization, *Eur. Polym. J*. 2020, **125**, 109503.
34. A. Al Mousawi, A. Arar, M. Ibrahim-Ouali, S. Duval, F. Dumur, P. Garra, J. Toufaily, T. Hamieh, B. Graff, D. Gigmes, J.-P. Fouassier, J. Lalevée, Carbazole-based compounds as photoinitiators for free radical and cationic polymerization upon near visible light illumination, *Photochem. Photobiol. Sci*. 2018, **17**, 578-585.
35. A. Al Mousawi, D. Magaldi Lara, G. Noirbent, F. Dumur, J. Toufaily, T. Hamieh, T.-T. Bui, F. Goubard, B. Graff, D. Gigmes, J.-P. Fouassier, J. Lalevée, Carbazole derivatives with thermally activated delayed fluorescence property as photoinitiators/photoredox catalysts for LED 3D printing technology, *Macromolecules* 2017, **50**, 4913-4926.
36. A. Al Mousawi, F. Dumur, J. Toufaily, T. Hamieh, B. Graff, D. Gigmes, J.-P. Fouassier, J. Lalevée, Carbazole scaffold based photoinitiators/photoredox catalysts for new LED projector 3D printing resins, *Macromolecule*s 2017, **50**, 2747-2758.
37. J. Zhang, D. Campolo, F. Dumur, P. Xiao, D. Gigmes, J.-P. Fouassier, J. Lalevée, The carbazole-bound ferrocenium salt as a specific cationic photoinitiator upon near-UV and visible LEDs (365–405 nm), *Polym. Bull*. 2016, **73**, 493-507.
38. D. Anandkumar, S. Ganesan, P. Rajakumar, P. Maruthamuthuc, Synthesis, photophysical and electrochemical properties and DSSC applications of triphenylamine chalcone dendrimers via click chemistry. *New. J. Chem*. 2017, **41**(19), 11238-11249.

39. M. Planells, A. Abate, D.J. Hollman, S.D. Stranks, V. Bharti, J. Gaur, D. Mohanty, S. Chand, H.J. Snaith, N. Robertson, Diacetylene bridged triphenylamines as hole transport materials for solid state dye sensitized solar cells. *J. Mater. Chem. A.* 2013, **1**(23), 6949-6960.
40. Z.Q. Liang, X.M. Wang, G.L. Dai, C.Q. Ye, Y.Y. Zhou, X.T. Tao, The solvatochromism and aggregation-induced enhanced emission based on triphenylamine-propenone. *New. J. Chem*. 2015, **39**(11), 8874-8880
41. F. Dumur, F. Goubard, Triphenylamines and 1,3,4-oxadiazoles: a versatile combination for controlling the charge balance in organic electronics, *New J. Chem*. 2014, **38**, 2204-2224.
42. M. Jin, M. Yu, Y. Zhang, D. Wan, H. Pu, 2,2,2-trifluoroacetophenone-based D-π-A type photoinitiators for radical and cationic photopolymerizations under near-UV and visible LEDs. *J. Polym. Sci., Part A: Polym. Chem*. 2016, **54**, 1945-1954.
43. R. Da Costa, F. Farias, L. Maqueira, C. Castanho Neto, L. Carneiro, J. Almeida, C. Buarque, R. Aucélio, J. Limberger, Synthesis, Photophysical and Electrochemical Properties of Novel D-π-D and D-π-A Triphenylamino-Chalcones and β-Arylchalcones. *J. Braz. Chem. Soc*. 2019, **30**(1), 81-89.
44. S. Dadashi-Silab, S. Doran, Y. Yagci, Photoinduced Electron Transfer Reactions for Macromolecular Syntheses. *Chem. Rev.* 2016, **116** (17), 10212-10275.
45. G. Chen, H.Y. Wang, Y. Liu, X.P. Xu, S.J. Ji, The synthesis and characterisation of novel pyrazoline derivatives containing triphenylamine, *Dyes Pigm*. 2010, **85**, 194-200.
46. K. Sun, K.; Y.Y. Xu, F. Dumur, F. Morlet-Savary, H. Chen, C. Dietlin, B. Graff, J. Lalevee, P. Xiao, In silico rational design by molecular modeling of new ketones as photoinitiators in three-component photoinitiating systems: application in 3D printing. *Polym. Chem*., 2020, **11**(12), 2230-2242.
47. J. Zhang, S.H. Wang, J. Lalevée, F. Morlet-Savary, E.S.H. Lam, B. Graff, J. Liu, F.Y. Xing, P. Xiao, 1,2-Diketones as Photoinitiators of both cationic and free-radical photopolymerization under UV (392 nm) or Blue (455 nm) LEDs. *J. Polym. Sci*. 2020, **58**, 792-802.
48. D.R. Duling, Simulation of multiple isotropic spin-trap EPR spectra. *J. Magn. Reson*. 1994, **104**(2), 105-110.
49. N.C. Padmavathi, P.R. Chatterji, Structural characteristics and swelling behavior of poly(ethylene glycol) diacrylate hydrogels. *Macromolecules* 1996, **29**(6), 1976-1979.
50. S.L. Gaonkar, U.N. Vignesh, Synthesis and pharmacological properties of chalcones: a review. *Res. Chem. Intermediat.* 2017, **43**, 6043–6077.
51. M.A. Tehfe, J. Lalevée, F. Morlet-Savary, B. Graff, N. Blanchard, J.-P. Fouassier, Tunable organophotocatalysts for polymerization reactions under visible lights. *Macromolecules* 2012, **45**, 1746-1752.
52. M. Abdallah, D. Magaldi, A. Hijazi, B. Graff, F. Dumur, J.-P. Fouassier, T.T. Bui, F. Goubard, J. Lalevée, Development of new high-performance visible light

photoinitiators based on carbazole scaffold and their applications in 3d printing and photocomposite synthesis. *J. Polym. Sci. A Polym. Chem*. 2019, **57** (20), 2081-2092.
53. A.A. Pawar, S. Halivni, N. Waiskopf, Y. Ben-Shahar, M. Soreni-Harari, S. Bergbreiter, U. Banin, S. Magdassi, Rapid three-dimensional printing in water using semiconductor–metal hybrid nanoparticles as photoinitiators. *Nano Letters* 2017; **17** (7), 4497-4501.
54. J. Niu, D.J. Lunn, A. Pusuluri, J.I. Yoo, M.A. OQMalley, S. Mitragotri, H.T. Soh, C.J. Hawker, Engineering live cell surfaces with functional polymers via cytocompatible controlled radical polymerization. *Nature Chem*. 2017, **9**, 537.
55. Z.H. Zhang, N. Corrigan, A. Bagheri, J.Y. Jin, C. Boyer, A versatile 3D and 4D printing system through photocontrolled RAFT polymerization. *Angew. Chem*. 2019, **131**, 18122-18131.
56. Y. Liu, Y. Li, G. Yang, X.T. Zheng, S.B. Zhou, Multi-stimulus-responsive shape-memory polymer nanocomposite network cross-linked by cellulose nanocrystals. *ACS Appl. Mater. Interf*. 2015, **7** (7), 4118-4126.

TOC graphic: